IOP Conference Series: Materials Science and Engineering

PURPOSE-LED PUBLISHING™

PAPER • **OPEN ACCESS**

Crystal structure, molecular mechanics and *In silico* analyses of piperizine derivative against human mammary carcinoma cells inhibition.

To cite this article: H Keshav Kumar *et al* 2024 *IOP Conf. Ser.: Mater. Sci. Eng.* **1300** 012007

View the article online for updates and enhancements.

You may also like

- Corrosion Behavior of Carbon Steel in Piperazine Solutions for Post-Combustion CO_2 Capture
Liangfu Zheng
- Preparation and Characterization of Impregnated Commercial Rice Husks Activated Carbon with Piperazine for Carbon Dioxide (CO_2) Capture
S N Masoum Raman, N A Ismail and S S Jamari
- Simple and green synthesis of piperazine-grafted reduced graphene oxide and its application for the detection of Hg(II)
Yinxiu Zuo, Jingkun Xu, Huakun Xing et al.

This content was downloaded from IP address 106.79.207.185 on 21/10/2024 at 07:40

Crystal structure, molecular mechanics and *In silico* analyses of piperizine derivative against human mammary carcinoma cells inhibition.

H Keshav Kumar[1], S Ananda[1], Dukanya[2], V Keerthikumara[1], Basappa[3], M Mahendra[1*]

[1]Department of Studies in Physics, University of Mysore, Manasagangotri, Mysuru 570 006, Karnataka.

[2] PG Department of Chemistry, JSS College for Women, Saraswathipuram, Mysuru 570 009, Karnataka.

[3]Department of Studies in Organic Chemistry, University of Mysore, Manasagangotri, Mysuru 570 006, Karnataka.

[*]**Corresponding author:** *mahendra@physics.uni-mysore.ac.in*

Abstract. In the present study, the single crystal of novel piperazine derivative4-(2, 3-chlorophenyl) piperazine-1-yl) (2-hydroxyphenyl) methanone (KDM) is grown by using the solvent evaporation method. The 3D structure of the molecule is confirmed by the single-crystal X-ray diffraction method. The study revealed that the molecular system is crystallized in the orthorhombic system with space group P_{bca}. The supramolecular crystal architecture establishes the stability of a compound *via* short contacts and halogen-hydrogen interactions. The Hirshfeld surface analysis were performed to evaluate the numerous intermolecular interactions based on the anisotropy of the topology. The Frontier molecular orbital (FMO) analysis and Molecular electrostatic potential (MEP) plots are investigated to understand the electronic structure properties of compounds using Density Functional Theory (DFT). *In silico* molecular docking, analysis is carried out to predict the best binding pose of the compound in the active site pocket of the BCl-XL/BAK protein-protein interface. Further, *in vitro* cytotoxicity studies against human breast cancer (MCF-7) cell lines of similarly designed piperazine-based derivatives showed prominent results. The results of the current study revealed that the compounds under investigation possess potential anti-cancer properties.

1.Introduction

Cancer treatment has remained dishearteningly low despite adopting multimodality therapy in the medical field. The 5-year survival rate typically ranges from 6% to 14% in males and 7% to 18% in females [1]. Targeted medications are aimed at oncogenic driving mutations in adenocarcinoma treatments and treatment with radiation, surgery, and chemotherapy [2].
Among the B-cell lymphoma (BCL) proteins' family, BCL-XL belongs to the family with anti-apoptotic function. It inhibits cell death by preventing the release of cytochrome c and apoptotic factors from the mitochondria into the cytoplasm. The release of apoptotic factors is a crucial step in initiating the cell death process. On the other hand, BCL-2-associated death promoter (BAK) is a pro-apoptotic that promotes cell death. When BAK is activated, it forms pores (channels) in the mitochondrial membrane, releasing cytochrome c with other apoptotic factors into the cytoplasm. The interaction between the BCL-XL and BAK is a critical aspect of the regulation of apoptosis, a process of programmed cell death that plays an significant role in tissue homeostasis maintainence and preventing the survival of damaged or abnormal cells [12]. When BCL-XL and BAK interact, BAK's pro-apoptotic activity can be neutralized by preventing apoptosis and blocking the cytochrome's release from the mitochondria and other apoptotic factors. These released factors activate caspases, which are proteases that initiate cellular

Content from this work may be used under the terms of the Creative Commons Attribution 3.0 licence. Any further distribution of this work must maintain attribution to the author(s) and the title of the work, journal citation and DOI.
Published under licence by IOP Publishing Ltd

destruction during apoptosis. Hence, the balancing between pro-apoptotic and anti-apoptotic BCL family proteins is crucial for determining whether a cell will undergo apoptosis or survive. Disruption of this balance, such as increase of expression in anti-apoptotic proteins or reduce of expression of pro-apoptotic proteins contributing to cancer development and resistance to cancer treatments.
A small molecule interaction with the interface of BCL-XL and BAK modulates the sensitive balance between cell survival and apoptosis. These interactions leads to implications for cellular function, tissue homeostasis, and disease processes, particularly in cancer therapy and the regulation of programmed cell death [13]. Scientists and biologists are continually intrigued by molecules with small molecular masses because of their propensity to significantly influence the operation of macromolecules that make up living systems. Small-molecule modifies the protein function and provides the framework for chemically changing the state of disease and 'probes' in chemical genetics to analyze biological systems [3, 4]. Among heterocyclics, piperazine is a significant bioactive natural product. It is precious in drug discovery across therapeutic applications, including antitumor, antibacterial, antifungal, and anti-Alzheimer medications [5]. Given this, we herein suggest a novel class of piperazine derivative for the inhibition of cancer cells and show its potential as a suitable candidate for drug development.

2.Experimental and Computational Methods

The block-shaped single crystal KDM having dimensions 0.21×0.24×0.32 cm was subjected to X-ray diffraction (XRD) using a Bruker D8 Diffractometer using Apex II CCD Detector equipped with monochromatic MoKα radiation (Wavelength λ = 0.7103 Å). The structure was further solved by direct methods and refined using SHELXS and SHELXL, respectively [6, 7]. The geometrical figures were generated and visualized by PLATON and MERCURY software [8]. The computational calculation was performed using the Gaussian 09 program [9] package at the B3LYP method level with a standard 6-311++ G(d, p) basis set. AutoDock Tools (ADT) (v1.5.7) [10] software package was employed to perform *in silico* molecular docking analysis.

3.Results and Discussions

3.1 Single Crystal Structure X-ray Analysis

The single crystal X-ray analysis unveiled the confirmation of 3D structure of the KDM in orthorhombic system with P_{bca} space group, respectively. The geometrical lattice parameters were found to be a=10.0827 Å, b= 13.0922 Å, c= 24.6781 Å, α =β =γ =90°, Volume (V) = 3257.6 Å^3 and Z= 8. The ORTEP view with a 50% probability of the KDM molecule is shown in Figure 1(a). The packing diagram of molecule along b-axis exhibited halogen mediated hydrogen bond interactions as shown in Figure 1(b). The halogen-hydrogen interactions are obsereved among atoms CL8…H3 and Cl7…H10A with 2.7 and 2.9Å, respectively. The KDM is also stabilized by C-H…O type inermolecular interactions.

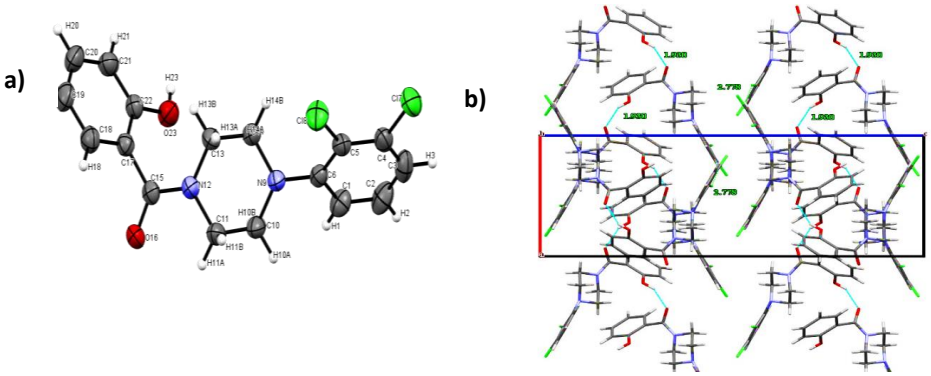

Figure 1: a) ORTEP drawn at 50% probability b) Packing diagram with halogen and hydrogen bond interactions along b-axis

3.2 *Hirshfeld Surface Analysis*

The packing modes investigations, intermolecular interaction, and molecular shape corresponding to the crystalline environment are explored using Hirshfeld surface analysis (Figure 2a). The information is obtained based on electron density distribution by mapping Hirshfeld surfaces with d_{norm}. The 2D fingerprint plots are generated by combining d_e and d_i distances with the help of Crystal Explorer 17.5 [11]. The fingerprint plots resulted in different regions of the area with H...H (38.2%), Cl-H…H-Cl (22.2%), C-H…H-C (20.2%), and O-H…H-O (12.7%) interactions (Figure 2c). The most noticed interaction in comparison is the H...H interaction, and the least is N-H…H-N (1.1%) interaction. The shape index diagram depicts the π-π interaction in the molecule encircled in black (Figure 2b).

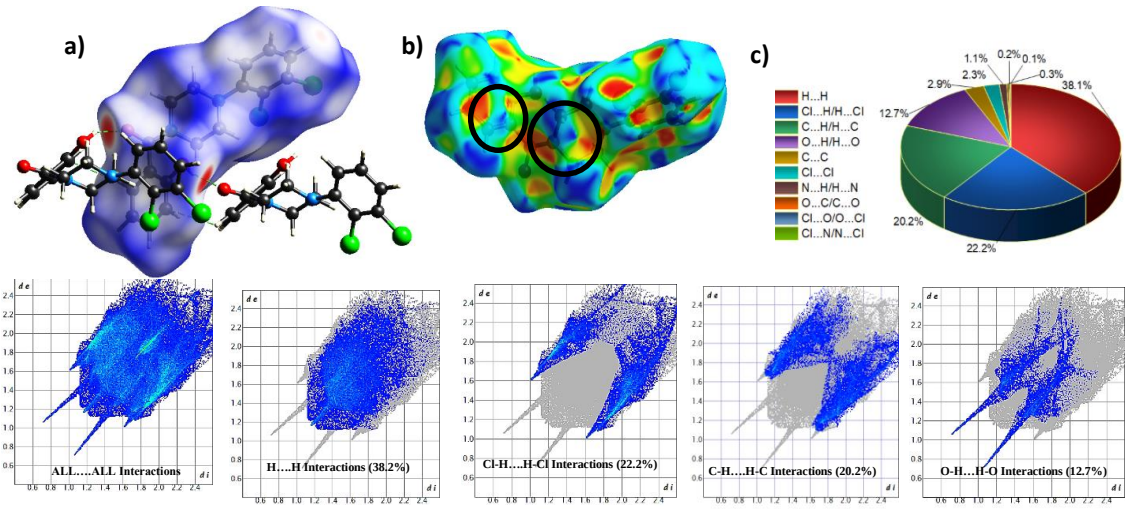

Figure 2 : a) Hirshfeld surface mapped with d_{norm} showing prominent interactions b) Shape index c) 2D Fingerprint plots showing percentage of intermolecular interactions

3.3.Density Functional Theory Calculations

3.3.1 Frontier Molecular Orbital (FMO) and Molecular Electrostatic Potential (MEP) Analysis

The quantum chemical characteristics of the highest occupied molecular orbital (HOMO) and the lowest unoccupied molecular orbital (LUMO) show the donation and acceptance of electrons, respectively. The computations are carried out using basis level theory B3LYP/6-311++G (d, p). The physicochemical properties, such as kinetic stability, chemical hardness/softness, and reactivity of the molecule, are characterized by the HOMO-LUMO energy gap (Table 1). The HOMO and LUMO orbitals of the KDM molecule are shown in Figure 3. The energy gap is found to be 4.744eV. The electronegativity and electrophilicity of KDM are observed to be 2.831 and 3.672 eV, respectively. The MEP plot was employed to understand the molecule's predicted reactive sites, such as electrophilic or nucleophilic sites. An electron isosurface map with an electrostatic potential surface indicates the molecule's size, shape, charge density, and reactive sites. Figure 4 depicts the resulting MEP map of the KDM compound.

Table 1 : Global Chemical Reactivity Descriptor Parameters

Molecule Properties	KDM
Energy in a. u.	-1838.07
E_{HOMO} in eV	-6.044
E_{LOMO} in eV	-1.300
$\Delta E_{LUMO-HOMO}$ in eV	4.744
Ionization potential (I)	6.044
Electron affinity (A)	1.300
Global Hardness (η)	2.372
Softness (S)	0.210
Chemical potential (μ)	-3.672
Electronegativity (χ)	3.672
Electrophilicity (ψ)	2.831

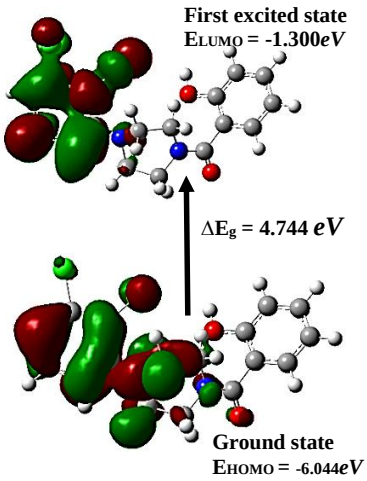

Figure 3: Frontier molecular orbital (FMO) plot

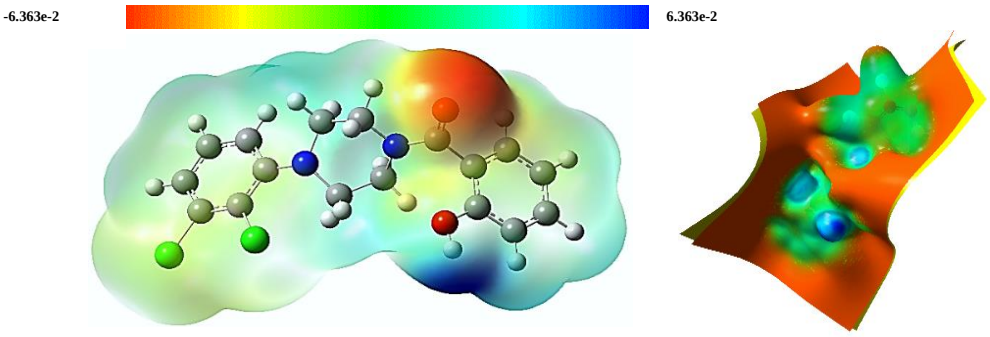

Figure 4: Molecular electrostatic potential (MEP) plot

3.4.In Silico Molecular Docking Analysis

In silico molecular docking, the analysis determined the optimal binding pose of the KDM molecule in the active site B-cell lymphoma-extra-large (BCL-XL) and BCL-2-associated death promoter (BAK) protein-protein interface. The crystal structure of BCL-XL bounded to BAK was downloaded from the RCSB Protein data bank having PDB ID: 5fmk (https://www.rcsb.org/). Figure 5 illustrates the binding pose of the KDM at the binding site BCL-XL/BAK interface, along with various interactionsbetween neighbouring aminoacids. The binding energy resulted in -8.5 kcal/mol having an inhibition constant value of 1.56 μM. The interaction formed a strong hydrogen bonding between the O-H group and GLU129 and ASP133 amino acids, respectively, having bond lengths of 1.98Å and 1.92Å. The KDM exhibited hydrophobic interactions among ARG132, PHE131, LEU 130, VAL126 and GLU129 amino acids. Further π-π stacking interactions were obsereved between piperizne and dichloro benzene ring moieties with LEU130 and VAL126, respectively. As a result,the molecule binds effectively with BCL-XL. Therefore, the synthetic KDM effectively inhibits BAK phosphorylation in BCL-XL, preventing cancer cell proliferation. Based on the core structural geometry of KDM, Girimanchanaika et al.,

reported the design and synthesis of eighteen molecules and were further sent for cytotoxic studies against MCF-7 cell lines, which showed prominent anti-cancer activities [12].

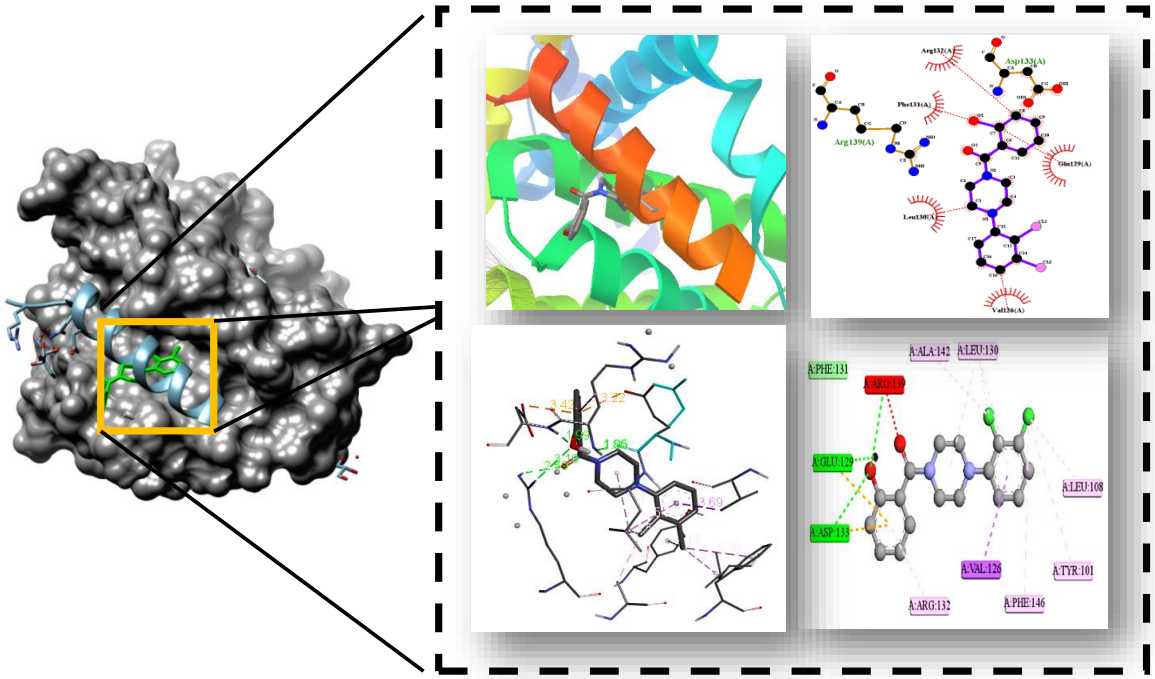

Figure 5: Binding interactions of KDM with BCL-XL protein at the binding site associated with BAK protein

Conclusion

The three-dimensional crystal structure of 4-(2, 3-chlorophenyl) piperazine-1-yl) (2-hydroxyphenyl) methanone (KDM) is determined using a single X-ray diffraction technique. The compound resulted in prominent hydrogen bond interactions in the experiment and DFT. Frontier molecular orbital (FMO) and molecular electrostatic potential (MEP) analyses of KDM were performed by DFT at the B3LYP/6311++G (d, p) basis set to understand the chemical reactive sites and global descriptor parameters of the compound. The KDM was firmly bound into the BCL-XL/BAK interface pocket, which deserves a potential candidate for cancer cell growth inhibition.

Acknowledgments

The author, Keshav Kumar H., would like to thank the Sophisticated Analytical Instrumentation Facility (SAIF), IIT Madras, for the SCXRD facility.

References

[1] Youlden, D. R., Cramb, S. M.,and Baade, P. D. (2008). The International Epidemiology of Lung Cancer: geographical distribution and secular trends. *Journal of thoracic oncology*, *3*(8), 819-831.
[2] Zhang, M., Wang, B., and Lobie, P. E. (2019). A novel small-molecule inhibitor of trefoil factor 3 (TFF3) potentiates MEK1/2 inhibition in lung adenocarcinoma. *Oncogenesis*, *8*(11), 65.
[3] Spring, D. R. (2005). Chemical genetics to chemical genomics: small molecules offer big insights. *Chemical Society Reviews*, *34*(6), 472-482.

[4] Kawasumi, M., and Nghiem, P. (2007). Chemical genetics: elucidating biological systems with small-molecule compounds. *Journal of investigative dermatology*, *127*(7), 1577-1584.
[5] Zhang, R. H., Guo, H. Y., and Quan, Z. S. (2021). Piperazine skeleton in the structural modification of natural products: a review. *Journal of enzyme inhibition and medicinal chemistry*, *36*(1), 1165-1197.
[6] Bruker, A. X. S. Inc. (2004) APEX 2. Bruker Advanced X-ray Solutions, Madison, Wisconsin, USA.
[7] Sheldrick, G. M. (2015). Crystal structure refinement with SHELXL. *Acta Crystallographica Section C: Structural Chemistry*, *71*(1), 3-8.
[8] Spek, A. L. (1990). PLATON, is an integrated tool for the analysis of the results of a single crystal structure determination. *Acta Crystallographica Section A: Foundations of Crystallography*, 46(s1), c34-c34
[9] Gaussian 09, Revision A.02, M. J. Frisch Gaussian, Inc., Wallingford CT, 2016.
[10] Morris, G. M., Huey, R., Lindstrom, W., Sanner, M. F., Belew, R. K., Goodsell, D. S. and Olson, A. J. (2009) Autodock4 and AutoDockTools4: automated docking with selective receptor flexibility. *J. Computational Chemistry* 2009, **16**: 2785-91.
[11] Turner, M. J., McKinnon, J. J., Wolff, S. K., Grimwood, D. J., Spackman, P. R., Jayatilaka, D., and Spackman, M. A. (2017). CrystalExplorer17.
[12] Girimanchanaika, S. S., Dukanya, D., Swamynayaka, A., Govindachar, D. M., Madegowda, M., Periyasamy, G and Basappa, B. (2021). Investigation of npb analogs that target phosphorylation of bad-ser99 in human mammary carcinoma cells. *International Journal of Molecular Sciences*, *22*(20), 11002.
[13] Pandey, V., Wang, B., Mohan, C. D., Raquib, A. R., Rangappa, S., Srinivasa, V., and Lobie, P. E. (2018). Discovery of a small-molecule inhibitor of specific serine residue BAD phosphorylation. *Proceedings of the National Academy of Sciences*, 115(44), E10505-E10514.